Optics Letters

Sensing of triglyceride concentration in blood solution using photoacoustic microscopy

Nan Wan,[1] Zhe Li,[2] Myeongsu Seong,[3] Ke Zhang,[1] Wei Niu,[4] Rong Wu,[5] and Sung-Liang Chen[1,6,7,*]

[1]University of Michigan-Shanghai Jiao Tong University Joint Institute, Shanghai Jiao Tong University, Shanghai 200240, China
[2]Department of Critical Care Medicine, Renji Hospital School of Medicine, Shanghai Jiao Tong University, Shanghai 200127, China
[3]Research Center for Intelligent Information Technology, Nantong University, Nantong 226019, China
[4]Department of Nephrology, Huadong Hospital Affiliated to Fudan University, Shanghai 200040, China
[5]Department of Ultrasound, Shanghai General Hospital, Shanghai Jiao Tong University School of Medicine, Shanghai 200080, China
[6]Engineering Research Center of Digital Medicine and Clinical Translation, Ministry of Education, Shanghai 200030, China
[7]State Key Laboratory of Advanced Optical Communication Systems and Networks, Shanghai Jiao Tong University, Shanghai 200240, China
*sungliang.chen@sjtu.edu.cn

Received 8 January 2023; revised 18 May 2023; accepted 22 May 2023; posted 25 May 2023; published 11 July 2023

The level of triglyceride (TG) in blood is essential to human health, and hypertriglyceridemia (TG level > 150 mg/dL) would lead to cardiovascular disease and acute pancreatitis that threaten human life. Routine methods for measuring the TG level in blood depend on a lipid panel blood test, which is invasive and not convenient. Here, we use photoacoustic (PA) microscopy to test the PA amplitude of blood solutions (based on hemoglobin powder as well as flowing sheep blood) with different TG concentrations. Interestingly, we observe that the PA amplitude increases with increasing TG concentration in blood solutions, which is attributed to the increase of the Grüneisen coefficient. The preliminary *in vitro* study shows that the PA methodology is able to detect the TG level down to 450 mg/dL. This finding provides an opportunity for using photoacoustics to noninvasively diagnose hypertriglyceridemia.

https://doi.org/10.1364/OL.485194

The level of blood lipid, which mainly consists of triglyceride (TG), high density lipoprotein cholesterol (HDL-C), and low-density lipoprotein cholesterol (LDL-C), is of great importance to the health status of the human body. Hypertriglyceridemia (TG level > 150 mg/dL) results in a high risk of cardiovascular disease [1,2]. In addition, severe hypertriglyceridemia (TG level > 1000 mg/dL) would increase both the risk of cardiovascular events and the risk of acute pancreatitis [3,4], and threatens human life.

Typically, the TG level in blood is measured and determined by a lipid panel blood test [5,6], which requires blood draw and brings tingling sensations. Thus, it is not convenient for routine monitoring and decreases the desire for examination of potential patients. Whereafter, hospitals or specialized laboratories would spend at least several hours reporting the results based on biochemical analysis, which may also delay the treatment. Therefore, development of a noninvasive, convenient, and rapid method to sense the concentration of TG in blood is urgently needed.

Optical imaging techniques are often developed and employed to noninvasively measure the physical signs for health monitoring and disease diagnosis [7,8]. Among them, photoacoustic (PA) imaging (PAI), which combines high optical contrast based on optical absorption and large penetration depth of ultrasound detection, has drawn increasing attention and has been widely studied in recent years [9]. PAI can be divided into three categories, PA computed tomography (PACT), acoustic-resolution PA microscopy (PAM) (AR-PAM), and optical-resolution PAM (OR-PAM) [10,11]. With PAI, subcutaneous vessel imaging [12], breast tumor imaging [13,14], oxygen saturation (sO_2) mapping [15,16], and melanoma imaging can be realized [17,18]. Some works also report that PAI can be used to probe the lipid content, based on the illumination of laser light at the wavelength around 1210 nm; however, most of them are limited to imaging of the lipid content in subcutaneous tissue [19] or imaging of the lipid-rich plaque [20,21], while there has been no study about using PAI to measure the blood lipid concentration, especially TG concentration in blood.

In this work, we use AR-PAM with excitation wavelengths of 532 nm and 797 nm, to investigate PA signals of the blood solutions [based on hemoglobin (Hb) powder as well as flowing sheep blood] with different TG concentrations. Then, we investigate the underlying principle of why PA amplitude increases with increasing TG concentration in blood solutions with fixed Hb concentration. At the excitation wavelength, the optical absorption predominantly comes from Hb rather than TG (e.g., at 532 nm, the absorption coefficient of Hb is four orders of magnitudes larger than that of TG [22]). Thus, if we find some differences in the PA amplitude, it would not be due to the difference in the optical absorption from blood solutions with fixed Hb concentration and with different TG concentration. By analyzing the PA amplitude of blood solutions with different TG concentration, interestingly, we find that the PA amplitude increases with increasing TG concentration in blood solutions with fixed Hb concentration, which may be attributed to the increase of the Grüneisen coefficient. This finding provides an

opportunity for using photoacoustics to noninvasively measure the TG concentration in blood.

We mainly conducted two experiments using blood solutions based on Hb powder as well as flowing sheep blood. For the first experiment, we prepared seven blood solutions, each of them consisting of Hb, TG, and de-ionized (DI) water, for the *in vitro* imaging experiment. Specifically, Hb lyophilized powder (R010156, Rhawn) was first dissolved in DI water, and then seven different amounts of TG (Structural Fat Emulsion Injection, Fresenius Kabi Ltd.) were added to form the final blood solutions with different TG concentration. In the seven blood solutions, the Hb concentration is kept as 150 mg/mL (normal Hb concentration in blood) [23,24], while the TG concentration is set as 0 mg/dL, 150 mg/dL, 450 mg/dL, 1000 mg/dL, 2000 mg/dL, 4500 mg/dL, and 9000 mg/dL. Whereafter, seven spotting capillary tubes (inner diameter, 500 μm; outer diameter, 700 μm) filled with the seven blood solutions were fixed on a cover glass side by side, and then they were placed into the water tank for imaging experiments. Note that the two ends of the capillary tubes were sealed, and the sealed capillary tubes were immersed in water to facilitate acoustic coupling. In total, eight repeated experiments were performed. That is, 8×7 tubes of blood solutions were made, and PAI was then performed eight times to obtain reliable results. Note that 150 mg/dL is the upper limit of normal TG level in blood.

For the second experiment, defibrillated sheep blood samples (Shanghai Yuanye Biotechnology Co., Ltd., China) were used. Specifically, four samples were prepared with different TG concentrations, which are denoted as Samples 1–4. For Sample 1, the bought sheep blood sample was used. Then, Samples 2–4 were prepared to have a TG level of 300 mg/dL, 850 mg/dL, and 1850 mg/dL higher than that of Sample 1, respectively. A peristaltic pump flow system (One China Road Fluid Technology Co., Ltd., China) was used for sample flowing. The rotation speed of the pump flow system was set as 300 rpm, and a silicone tube with an inner diameter of 1.8 mm and an outer diameter of 2.2 mm was used to transport the four blood samples in turn. The sample preparation and PA signal acquisition for the flowing sheep blood experiment are detailed in Section 1 of Supplement 1.

A homebuilt AR-PAM system (Fig. 1) was employed to acquire PA signals and images. In the AR-PAM system, a 6-ns pulsed laser (Qsmart 450, Quantel) with pulse repetition frequency of 20 Hz and wavelength of 532 nm was used for PA

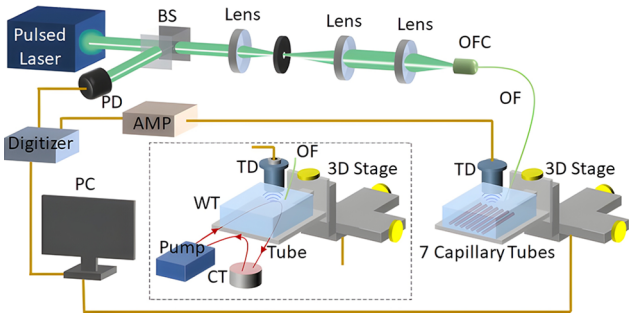

Fig. 1. Schematic of the AR-PAM imaging system for *in vitro* imaging of blood solutions with different TG concentrations. Inset shows a pump flow system for the flowing sheep blood experiment. BS, beam splitter; PD, photodetector; AMP, preamplifier; OF, optical fiber; OFC, optical fiber coupler; TD, transducer; PC, personal computer; WT, water tank; CT, container.

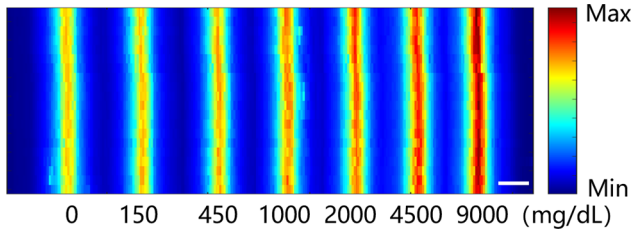

Fig. 2. One representative PAM image of the seven blood solutions with different TG concentrations (0 mg/dL, 150 mg/dL, 450 mg/dL, 1000 mg/dL, 2000 mg/dL, 4500 mg/dL, and 9000 mg/dL). Scale bar: 200 μm.

excitation for the first experiment, and another pulsed laser (Spitlight EVO200 OPO Midband, InnoLas, Germany) that provides excitation wavelength of 797 nm was used for the second experiment. The laser was coupled into a multimode optical fiber (MHP910L02, Thorlabs). A focused ultrasonic transducer was used to receive PA signals. The focused transducer was made by attaching an acoustic lens (45006, Edmund Optics, NJ) to a 50-MHz flat ultrasonic transducer (V214-BC-RM, 77% bandwidth, Panametrics NDT, MA), which provides a numerical aperture of 0.44 and a focal length of 6.7 mm. During image acquisition, the imaging head of AR-PAM, consisting of the optical fiber and the focused transducer, was fixed with a motorized stage (not shown in Fig. 1) for scanning. The sample was immersed in a water tank, which can be adjusted by a three-dimensional (3D) stage. Detected PA signals were amplified by a low-noise preamplifier (ZFL-500LN+, Mini-Circuits), recorded by a digitizer (CSE1422, Gage), and then stored in a computer. The lateral and axial resolution of the AR-PAM system was approximately 65 μm and 40 μm, respectively [25]. The inset of Fig. 1 shows the pump flow system to realize the flowing sheep blood for the flowing sheep blood experiment.

For the experiment using the blood solutions based on Hb powder, one representative PAM image (maximum amplitude projection along the depth direction) of the seven blood solutions with different TG concentrations (0 mg/dL, 150 mg/dL, 450 mg/dL, 1000 mg/dL, 2000mg/dL, 4500 mg/dL, and 9000 mg/dL) is shown in Fig. 2. We can see that the PA amplitude increases with increasing TG concentration.

For quantitative analysis, in the PAM images, the maximum pixel values along each row of each sample are recorded, and then the means and standard deviations of each sample can be calculated based on the abovementioned maximum pixel values. As mentioned previously, eight experiments were conducted and considered in the analysis. The mean PA amplitude of the blood solution with a TG concentration of 0 mg/dL is set as unity for normalization. That is, the mean PA amplitude of the blood solutions with different TG concentration is divided by that of the blood solution with TG concentration of 0 mg/dL. Then, the normalized mean PA amplitude is 1.0049, 1.0630, 1.1105, 1.2012, 1.3074, and 1.4186 for the blood solutions with TG concentrations of 150 mg/dL, 450 mg/dL, 1000 mg/dL, 2000 mg/dL, 4500 mg/dL, and 9000 mg/dL, respectively, as shown in Fig. 3. For statistical analysis, the results of every two adjacent TG concentrations are examined by *t*-test, and the *p*-values are all less than 0.0001 except the comparison between the TG concentrations of 0 mg/dL and 150 mg/dL, indicating that PAI can be used to detect a TG level >450 mg/dL. Note that the *p*-value for the comparison between the TG concentration of 0 mg/dL

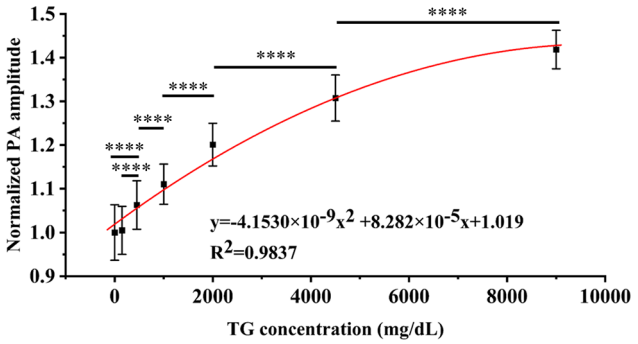

Fig. 3. Normalized PA amplitude increases with increasing TG concentration (0 mg/dL, 150 mg/dL, 450 mg/dL, 1000 mg/dL, 2000 mg/dL, 4500 mg/dL, and 9000 mg/dL) in the blood solutions based on Hb powder. Data are expressed as means ± standard deviations. ****, $p < 0.0001$.

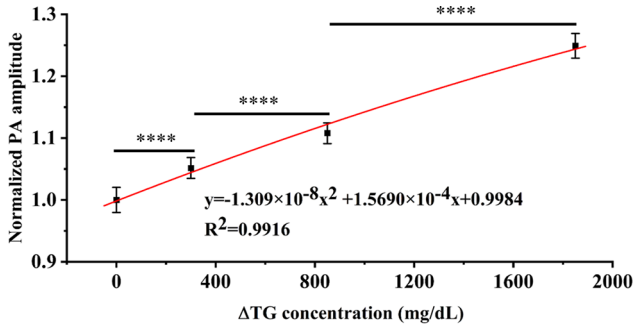

Fig. 4. Normalized PA amplitude increases with increasing ΔTG concentration [0 mg/dL (Sample 1), 300 mg/dL (Sample 2), 850 mg/dL (Sample 3), and 1850 mg/dL (Sample 4)] in the flowing sheep blood samples. Data are expressed as means ± standard deviations. ****, $p < 0.0001$.

and 450 mg/dL is also calculated, which is also less than 0.0001. The p-value for the comparison between the TG concentration of 0 mg/dL and 150 mg/dL is 0.444, indicating that they cannot be distinguished.

The initial PA pressure can be described by $P_0 = F\mu_a\Gamma$, where F is the optical fluence on the object, μ_a is the optical absorption of coefficient of the absorber, and Γ is the Grüneisen coefficient of the object [26]. In our experiments, optical fluence is kept the same. For optical absorption, all the seven blood solutions are with the same Hb concentration, and the optical absorption of Hb is four orders of magnitude larger than that of TG under the illumination laser wavelength of 532 nm. Therefore, the optical absorption of the seven blood solutions is considered the same, and the increased PA amplitude with increasing TG concentration in blood solutions (as observed in Figs. 2 and 3) should not be attributed to the factor of optical absorption. The verification that TG itself does not generate PA signals at an excitation wavelength of 532 nm is described in Section 2 and Fig. S1 of Supplement 1.

We believe the Grüneisen coefficient of the blood solutions is the key factor that causes the PA amplitude to increase with increasing TG concentration (Figs. 2 and 3). First, as discussed above, the optical fluence and optical absorption have been ruled out, and therefore, the Grüneisen coefficient is proposed to be responsible for the results in Figs. 2 and 3. Second, Laufer *et al.* suggested that the Grüneisen coefficient of solutions is linearly dependent on the solute concentration [27,28]. In this way, the Grüneisen coefficient of the blood solution increases with increasing TG concentration, which can explain the increased PA amplitude with increasing TG concentration in Fig. 3. That is, compared with the pure Hb solution, the increase of the Grüneisen coefficient can be estimated by the increased PA amplitude, which is 4.9%, 6.3%, 11.05%, 20.12%, 30.74%, and 41.86% for the blood solutions with TG concentrations of 150 mg/dL, 450 mg/dL, 1000 mg/dL, 2000 mg/dL, 4500 mg/dL, and 9000 mg/dL, respectively. Third, the Grüneisen coefficient can be expressed as $\Gamma = \beta v_S^2/C_p$ [9], where C_p is the specific heat that relates to light absorber Hb, v_s is acoustic speed, and β is volume expansion coefficient. Here, v_s and β relate to both TG and water, which are the surroundings of the light absorber Hb. The acoustic speeds v_s of TG and water are very close (1462.5 m/s for TG and 1482 m/s for water) [29,30], so the increase of TG concentration (along with the decrease of water concentration) would hardly cause an obvious change in the acoustic speed of the surroundings. A rough estimation gives <0.13% for the extreme case. However, the volume expansion coefficient β of TG is 7×10^{-4}/°C, which is approximately ~3.3 times larger than that of water (~2.14×10^{-4}/°C) (https://www.engineeringtoolbox.com/cubical-expansion-coefficients-d_1262.html). Therefore, the increase of TG concentration would increase the volume expansion coefficient of the surroundings around the light absorber Hb, which subsequently increases the Grüneisen coefficient of the blood solution and thus the PA amplitude. In Fig. 3, we observe that the increase of the normalized PA amplitude (or the Grüneisen coefficient) saturates at high TG concentration. A valid explanation regarding the saturation of the Grüneisen coefficient requires further investigation.

Further, a similar experiment using black ink as light absorber, to replace the light absorber Hb, was conducted, and a trend similar to that in Fig. 3 is observed. The experiment using black ink solutions is detailed in Section 3 and Fig. S2 of Supplement 1.

For the flowing sheep blood experiment, 100 B-scans were acquired for each sample. Similar to Figs. 2 and 3, the maximum pixel values for each B-mode image are recorded, and then the means and standard deviations of each sample can be calculated based on the abovementioned maximum pixel values. The mean PA amplitude of the four sheep blood samples is normalized to that of Sample 1. The normalized mean PA amplitude is 1, 1.0516, 1.1080, and 1.2492 for Samples 1–4, respectively, as shown in Fig. 4. As can be seen, a trend similar to that in Fig. 3 can still be observed. More discussion about the flowing sheep blood experiment and Fig. 4 (including the reasons to use an excitation wavelength of 797 nm) is described in Section 4 of Supplement 1.

Compared with the blood solutions based on Hb powder (Fig. 3), the flowing sheep blood model (Fig. 4) has more biological significance: (i) the sheep blood sample is more complicated and contains Hb, plasma, blood platelets, various proteins, antibodies, white blood cells, T cells, and neutrophils. The constituents of the sheep blood sample are close to human blood; (ii) the flowing sheep blood model is to mimic the blood flow in vessels, which is close to an *in vivo* environment for future clinical applications.

It is worth noting that similar trends (i.e., the PA amplitude increases with increasing TG concentration) are obtained using a

different light absorber (the blood solutions based on Hb powder in Fig. 3, the flowing sheep blood samples in Fig. 4, and the black ink solutions in Fig. S2). Thus, currently, we attribute the PA amplitude increases with increasing TG concentration in blood solutions to the increase of the Grüneisen coefficient, which, however, may not be the sole factor for the PA amplitude increases. Other factors, e.g., lipid aggregation or larger lipid particles with increasing TG concentration, may possibly contribute to the PA amplitude increases, which require further investigation in the future.

In the experiment using the blood solutions based on Hb powder, we set the TG concentration from 150 mg/dL to 9000 mg/dL, which is to mimic the different severity of hypertriglyceridemia in clinical scenarios. According to [31], moderate hypertriglyceridemia is designated for a TG level of 150–1000 mg/dL, and severe hypertriglyceridemia is designated for TG level of >1000 mg/dL. A more severe hypertriglyceridemia will result in a higher risk of cardiovascular events and acute pancreatitis [31]. A few cases of extremely high TG level have been reported [32,33], e.g., >10,000 mg/dL.

Although the linear dependence of the Grüneisen coefficient on the solute concentration was reported previously [27], considering the results in Figs. 3, 4, and S2 of Supplement 1 obtained in this work, we think it would be more reasonable to adopt a quadratic fit (i.e., a nonlinear fit) for our results.

In conclusion, we observed the phenomenon that PA amplitude increases with increasing TG concentration in blood solutions based on Hb powder as well as flowing sheep blood. Then, we investigated the underlying principle and attributed it to the Grüneisen coefficient. To the best of our knowledge, this is the first work that discusses the use of photoacoustics for the measurement of blood lipid. Toward clinical applications of noninvasive measurement of blood lipid using photoacoustics, much work needs to be further conducted. First, *ex vivo* experiments on sensing blood lipid with flowing human blood samples or *in vivo* experiments on sensing blood lipid with mouse and rabbit animal models should be performed to approach the realistic situation. Second, multi-wavelength PA quantitative spectroscopic measurement and data processing algorithm should be designed to overcome the interference from other molecule variations in blood, such as total Hb concentration and sO_2, and to improve the sensing specificity and sensitivity of blood lipid.

Funding. Natural Science Foundation of Shanghai (22ZR1428900); National Natural Science Foundation of China (61775134, 62235013, 82130057).

Disclosures. The authors declare no conflicts of interest.

Data availability. Data underlying the results presented in this paper are not publicly available at this time but may be obtained from the authors upon reasonable request.

Supplemental document. See Supplement 1 for supporting content.

REFERENCES

1. M. A. Austin, J. E. Hokanson, and K. L. Edwards, Am. J. Cardiol. **81**, 7B (1998).
2. A. Tenenbaum, R. Klempfner, and E. Z. Fisman, Cardiovasc. Diabetol. **13**, 159 (2014).
3. A. L. Yang and J. McNabb-Baltar, Pancreatology **20**, 795 (2020).
4. R. Garg and T. Rustagi, BioMed Res. Int. **2018**, 1 (2018).
5. A. Plüddemann, M. Thompson, C. P. Price, J. Wolstenholme, and C. Heneghan, Br. J. Gen. Pract. **62**, e224 (2012).
6. M. Sampson, A. Wolska, R. Warnick, D. Lucero, and A. T. Remaley, Clin. Chem. (Washington, DC, U. S.) **67**, 987 (2021).
7. H. Zhu, S. O. Isikman, O. Mudanyali, A. Greenbaum, and A. Ozcan, Lab Chip **13**, 51 (2013).
8. K. Licha and C. Olbrich, Adv. Drug Delivery Rev. **57**, 1087 (2005).
9. M. Xu and L. V. Wang, Rev. Sci. Instrum. **77**, 041101 (2006).
10. L. V. Wang and J. Yao, Nat. Methods **13**, 627 (2016).
11. J. Yao and L. V. Wang, Laser Photonics Rev. **7**, 758 (2013).
12. J. W. Baik, J. Y. Kim, S. Cho, S. Choi, J. Kim, and C. Kim, IEEE Trans. Med. Imaging **39**, 975 (2020).
13. L. Lin, P. Hu, J. Shi, C. M. Appleton, K. Maslov, L. Li, R. Zhang, and L. V. Wang, Nat. Commun. **9**, 2352 (2018).
14. L. Lin, X. Tong, P. Hu, M. Invernizzi, L. Lai, and L. V. Wang, Adv. Sci. **8**, 2003396 (2021).
15. T. Mitcham, H. Taghavi, J. Long, C. Wood, D. Fuentes, W. Stefan, J. Ward, and R. Bouchard, Photoacoustics **7**, 47 (2017).
16. C. Liu, Y. Liang, and L. Wang, Photoacoustics **17**, 100156 (2020).
17. Y. Zhou, W. Xing, K. I. Maslov, L. A. Cornelius, and L. V. Wang, Opt. Lett. **39**, 4731 (2014).
18. R. M. Weight, J. A. Viator, P. S. Dale, C. W. Caldwell, and A. E. Lisle, Opt. Lett. **31**, 2998 (2006).
19. Y. Cao, A. Kole, J. Hui, Y. Zhang, J. Mai, M. Alloosh, M. Sturek, and J.-X. Cheng, Sci. Rep. **8**, 2400 (2018).
20. K. Jansen, G. van Soest, and A. F. W. van der Steen, Ultrasound in Medicine & Biology **40**, 1037 (2014).
21. X. Ge, H. Cui, J. Kong, S. Y. Lu, R. Zhan, J. Gao, Y. Xu, S. Lin, K. Meng, L. Zu, S. Guo, and L. Zheng, Adv. Mater. **32**, 2000037 (2020).
22. T. J. Allen, A. Hall, A. P. Dhillon, J. S. Owen, and P. C. Beard, J. Biomed. Opt. **17**, 061209 (2012).
23. N. Bosschaart, G. J. Edelman, M. C. Aalders, T. G. van Leeuwen, and D. J. Faber, Lasers Med. Sci. **29**, 453 (2014).
24. C. Lee, K. Lim, S. S. Kim, L. X. Thien, E. S. Lee, K. T. Oh, H.-G. Choi, and Y. S. Youn, Colloids Surf., B **176**, 156 (2019).
25. D. Cai, Z. Li, Y. Li, Z. Guo, and S.-L. Chen, Opt. Express **25**, 1421 (2017).
26. L. V. Wang, IEEE J. Sel. Top. Quantum Electron. **14**, 171 (2008).
27. J. Laufer, E. Zhang, and P. Beard, IEEE J. Sel. Top. Quantum Electron. **16**, 600 (2010).
28. J. Laufer, B. Cox, E. Zhang, and P. Beard, Appl. Opt. **49**, 1219 (2010).
29. I. R. Gouw and I. R. Vlugter, Fette, Seifen, Anstrichm. **69**, 159 (1967).
30. V. A. Del Grosso and C. W. Mader, J. Acoust. Soc. Am. **52**, 1442 (1972).
31. K. G. Parhofer and U. Laufs, Deutsches Ärzteblatt International **116**, 825 (2019).
32. S. Irie, T. Anno, F. Kawasaki, R. Shigemoto, S. Nakanishi, K. Kaku, and H. Kaneto, BMC Endocr. Disord. **19**, 92 (2019).
33. A. Toor, A. Toor, K. Khalighi, and M. Krishnamurthy, Case Reports in Endocrinology **2019**, 6273196 (2019).